

GW-approximation energies and Hartree-Fock bands of semiconductors

R. Hott*

*Max-Planck-Institut für Festkörperforschung, Heisenbergstrasse 1, D-7000 Stuttgart 80,
Federal Republic of Germany*

(Received 29 January 1991)

GW-approximation calculations have been performed for diamond, silicon, germanium, gallium arsenide, and indium phosphide using refined numerical techniques. We obtained good but not perfect agreement of the *GW*-approximation energies with experiment. Exchange- and correlation-energy contributions and the Hartree-Fock bands of these substances have also been calculated.

I. INTRODUCTION

When band-structure calculations based on the local-density approximation^{1,2} (LDA) reached a stage of good convergence, it became clear that, in spite of the good description of the dispersion of the energy bands, the energy differences between conduction bands and valence bands in semiconductors and insulators calculated within the LDA scheme are in general too small compared with experiment.³

The central goal of this paper is to demonstrate how this can be improved by means of the so-called *GW approximation*.⁴⁻⁶ The principles of this method will be reviewed shortly in Sec. II. Section III shows the details of the method used for this work. Section IV compares the calculated *GW*-approximation energies with the corresponding LDA energies and experimental values for diamond, silicon, germanium, gallium arsenide, and indium phosphide. It also shows the contributions of exchange and correlation energies for these substances separately and the corresponding Hartree-Fock band structures. Section V gives a comparison with previous work. Finally, the paper concludes with a brief summary in Sec. VI.

II. PRINCIPLES OF THE CALCULATIONS IN GW APPROXIMATION

In the Green's-function technique, all one-particle properties can be obtained from the quasiparticle energies $\epsilon_{\mathbf{k}n}$ and the corresponding wave functions $\psi_{\mathbf{k}n}(\mathbf{r})$.⁷ These are the solutions of the quasiparticle equation

$$\begin{aligned} H\psi_{\mathbf{k}n}(\mathbf{r}) &= H_0\psi_{\mathbf{k}n}(\mathbf{r}) + \int d^3r' \Sigma(\mathbf{r}, \mathbf{r}'; \epsilon_{\mathbf{k}n})\psi_{\mathbf{k}n}(\mathbf{r}') \\ &= \epsilon_{\mathbf{k}n} \cdot \psi_{\mathbf{k}n}(\mathbf{r}), \end{aligned} \quad (1)$$

where the Hamiltonian H_0 includes the kinetic energy and the potential energy due to the ion cores and the valence electrons, and the self-energy operator Σ summarizes the many-body effects.

The Kohn-Sham equation²—the wave equation which has to be solved in the LDA scheme to obtain the *ground-state* properties—can be regarded as an approximation to

this quasiparticle equation where the self-energy operator is approximated by a *local and energy-independent* potential

$$\Sigma^{\text{LDA}}(\mathbf{r}, \mathbf{r}'; \epsilon) = V_{\text{xc}}^{\text{LDA}}(\mathbf{r}) \cdot \delta(\mathbf{r} - \mathbf{r}') . \quad (2)$$

This is constructed in such a way as to give an exact solution for the case of the homogeneous electron gas.⁸⁻¹⁰ The good agreement of LDA band structures and the *excitation* spectrum of solids is therefore somewhat unexpected.⁵ Nevertheless the agreement is not perfect, leading to several attempts to improve the LDA approximation of the self-energy (2).^{11,12}

A systematic way of constructing calculable approximations of the self-energy operator was initiated by Hedin.¹³ The simplest approximation within this scheme is the *GW approximation* (GWA): The self-energy

$$\begin{aligned} \Sigma^{\text{GWA}}(\mathbf{r}, \mathbf{r}'; \epsilon) &= \int_{\omega \in \mathbf{R}} d\omega \frac{e^{-i\omega 0^+}}{(-2\pi i)} G(\mathbf{r}, \mathbf{r}'; \epsilon - \omega) \\ &\quad \times W(\mathbf{r}, \mathbf{r}'; \omega) \end{aligned} \quad (3)$$

is approximated in GWA by a convolution with respect to the frequency variable of the Green's function

$$G(\mathbf{r}, \mathbf{r}'; \omega) = \sum_{(\mathbf{k}, n)} \frac{\psi_{\mathbf{k}n}(\mathbf{r})[\psi_{\mathbf{k}n}(\mathbf{r}')]^*}{\omega - \epsilon_{\mathbf{k}n} - i0^+(\epsilon_F - \epsilon_{\mathbf{k}n})} \quad (4)$$

with the *screened* Coulomb interaction W along the real axis. This led to the name of this approximation. ϵ_F denotes the Fermi energy.

The construction of Σ^{GWA} already includes the quasiparticle wave functions and energies. Therefore, the homogeneous electron gas was for a long time the only system where GWA results could actually be calculated.¹⁴ After some first attempts to apply the GWA to real systems¹⁵ Hybertsen and Louie⁴ proposed an iterative scheme for the calculation of the quasiparticle wave functions and energies by using its LDA counterparts as "starting values" for the computation. They claimed that they had already reached convergence after the first iteration, with excellent agreement of the LDA wave functions with the final quasiparticle wave functions

$$\psi_{\mathbf{k}n}(\mathbf{r}) \approx \psi_{\mathbf{k}n}^{\text{LDA}}(\mathbf{r}) \quad (5)$$

and very good agreement of the calculated energies with experimental energies.

III. DETAILS OF THE METHOD

The good agreement of the pseudofunctions¹⁶ used by Hybertsen and Louie with the wave functions calculated by the empirical pseudopotential method^{17,18} (EPM) is the basis of the method of von der Linden and Horsch⁶ for the calculation of energy *differences* between GWA and LDA. This method was used for the calculation of the GWA energies reported in this paper and will therefore be briefly reviewed including the technical improvements introduced by this work.

Choosing the norm and the overlap of the wave functions as

$$\int d^3r [\psi_{\mathbf{k}n}^{\text{LDA}}(\mathbf{r})]^* \psi_{\mathbf{k}n}^{\text{LDA}}(\mathbf{r}) = 1, \quad (6)$$

$$\int d^3r [\psi_{\mathbf{k}n}^{\text{LDA}}(\mathbf{r})]^* \psi_{\mathbf{k}n}(\mathbf{r}) = 1, \quad (7)$$

the quasiparticle equation (1) leads directly to

$$\begin{aligned} \epsilon_{\mathbf{k}n}^{\text{GWA}} - \epsilon_{\mathbf{k}n}^{\text{LDA}} &= \int d^3r \int d^3r' [\psi_{\mathbf{k}n}^{\text{LDA}}(\mathbf{r})]^* \\ &\quad \times [\Sigma^{\text{GWA}}(\mathbf{r}, \mathbf{r}'; \epsilon_{\mathbf{k}n}) \\ &\quad - \Sigma^{\text{LDA}}(\mathbf{r}, \mathbf{r}')] \psi_{\mathbf{k}n}(\mathbf{r}'). \end{aligned} \quad (8)$$

As the quasiparticle wave functions are expected to be approximated by the LDA wave functions in an excellent way in (5) $\psi_{\mathbf{k}n}(\mathbf{r})$ can be replaced by $\psi_{\mathbf{k}n}^{\text{LDA}}(\mathbf{r})$ to a good approximation. The superscript LDA for the wave functions will therefore be omitted from now on in this paper.

The expectation value of the LDA self-energy can then easily be evaluated:

$$\Sigma_{\mathbf{k}n}^{\text{LDA}} = \int d^3r [\psi_{\mathbf{k}n}(\mathbf{r})]^* V_{\text{xc}}^{\text{LDA}}(\mathbf{r}) \psi_{\mathbf{k}n}(\mathbf{r}). \quad (9)$$

The GWA part requires a much more complicated construction. First, the screened Coulomb interaction W has to be evaluated. This is most easily done using the Fourier representation:

$$\begin{aligned} W(\mathbf{r}, \mathbf{r}'; \omega) &= \frac{1}{V} \sum_{\mathbf{q}} \sum_{\mathbf{G}, \mathbf{G}'} e^{i(\mathbf{q}+\mathbf{G})\cdot\mathbf{r}} W_{\mathbf{G}\mathbf{G}'}(\mathbf{q}; \omega) \\ &\quad \times e^{-i(\mathbf{q}+\mathbf{G}')\cdot\mathbf{r}'}, \end{aligned} \quad (10)$$

$$W_{\mathbf{G}\mathbf{G}'}(\mathbf{q}; \omega) = \epsilon_{\mathbf{G}\mathbf{G}'}^{-1}(\mathbf{q}; \omega) \frac{4\pi e^2/V}{|\mathbf{q}+\mathbf{G}| \cdot |\mathbf{q}+\mathbf{G}'|}. \quad (11)$$

Within the GWA screening is described by the dielectric matrix^{19,20}

$$\epsilon_{\mathbf{G}\mathbf{G}'}(\mathbf{q}; \omega) = \delta_{\mathbf{G}\mathbf{G}'} - 4\pi e^2/V \sum_{\mathbf{k}} P_{\mathbf{G}\mathbf{G}'}(\mathbf{k}, \mathbf{q}; \omega), \quad (12)$$

where the polarization

$$\begin{aligned} P_{\mathbf{G}\mathbf{G}'}(\mathbf{k}, \mathbf{q}; \omega) &= \sum_{\substack{m:\text{val} \\ n:\text{con}}} M_{\mathbf{G}}^{mn}(\mathbf{k}, \mathbf{q}) \cdot [M_{\mathbf{G}'}^{mn}(\mathbf{k}, \mathbf{q})]^* \\ &\quad \times f(\epsilon_{\mathbf{k}+\mathbf{q},n} - \epsilon_{\mathbf{k},m}, \omega) \end{aligned} \quad (13)$$

is expressed in terms of matrix elements of the momentum operator

$$\begin{aligned} M_{\mathbf{G}}^{mn}(\mathbf{k}, \mathbf{q}) &= \frac{1}{|\mathbf{q}+\mathbf{G}|} \int d^3r [\psi_{\mathbf{k}m}(\mathbf{r})]^* e^{-i(\mathbf{q}+\mathbf{G})\cdot\mathbf{r}} \\ &\quad \times \psi_{\mathbf{k}+\mathbf{q}n}(\mathbf{r}) \end{aligned} \quad (14)$$

multiplied by

$$f(\epsilon, \omega) = \left(\frac{1}{\epsilon - \omega - i0^+} + \frac{1}{\epsilon + \omega + i0^+} \right). \quad (15)$$

The band index m runs over all (occupied) valence, n over all (empty) conduction bands. For the calculation of the frequency integral in the evaluation of the GWA self-energy expression (3) we parametrize the frequency dependence of the screened Coulomb interaction W — or equivalently of the dielectric function — by means of a *plasmon-pole* function.

Following von der Linden und Horsch,⁶ the dielectric matrix is determined using the concept of the *dielectric band structure*.^{21,22}

The static dielectric matrix $\epsilon_{\mathbf{G}\mathbf{G}'}(\mathbf{q}; \omega = 0)$ is a Hermitian matrix in the reciprocal lattice vector indices and can therefore be diagonalized yielding the dielectric band structure representation

$$\epsilon_{\mathbf{G}\mathbf{G}'}(\mathbf{q}; \omega = 0) = \sum_{\ell} \phi_{\mathbf{G}}^{\ell}(\mathbf{q}) \lambda_{\mathbf{q}\ell} [\phi_{\mathbf{G}'}^{\ell}(\mathbf{q})]^*. \quad (16)$$

The orthonormal eigenvectors $\phi_{\mathbf{G}}^{\ell}(\mathbf{q})$ are assumed to be frequency independent and the eigenvalues are approximated by the plasmon-pole form as

$$\begin{aligned} \lambda_{\mathbf{q}\ell}(\omega) &= \left[1 + \frac{z_{\mathbf{q}\ell}\omega_{\mathbf{q}\ell}}{2} \left(\frac{1}{\omega - (\omega_{\mathbf{q}\ell} - i0^+)} \right. \right. \\ &\quad \left. \left. - \frac{1}{\omega + (\omega_{\mathbf{q}\ell} - i0^+)} \right) \right]^{-1}. \end{aligned} \quad (17)$$

The plasmon-pole parameters, in turn, are determined by the eigenvalues calculated for $\omega = 0$,

$$z_{\mathbf{q}\ell} = [1 - \lambda_{\mathbf{q}\ell}(\omega = 0)]^{-1} \quad (18)$$

and by means of the f -sum rule²³

$$\begin{aligned} \omega_{\mathbf{q}\ell}^2 &= \frac{\omega_{\text{p1}}^2}{z_{\mathbf{q}\ell}} \sum_{\mathbf{G}, \mathbf{G}'} [\phi_{\mathbf{G}}^{\ell}(\mathbf{q})]^* \frac{(\mathbf{q}+\mathbf{G}) \cdot \bar{\rho}(\mathbf{G}-\mathbf{G}')}{|\mathbf{q}+\mathbf{G}|} \frac{(\mathbf{q}+\mathbf{G}')}{\bar{\rho}(0)} \frac{(\mathbf{q}+\mathbf{G}')}{|\mathbf{q}+\mathbf{G}'|} \\ &\quad \times \phi_{\mathbf{G}'}^{\ell}(\mathbf{q}). \end{aligned} \quad (19)$$

$\bar{\rho}(\mathbf{G})$ is the Fourier transform of the electron density and $\omega_{\text{p1}} = [\bar{\rho}(0)4\pi e^2/m]^{1/2}$ denotes the plasma frequency.²⁴

The expectation value of the GWA self-energy

$$\Sigma_{\mathbf{k}m}^{\text{GWA}} = \int d^3r \int d^3r' [\psi_{\mathbf{k}m}(\mathbf{r})]^* \Sigma^{\text{GWA}}(\mathbf{r}, \mathbf{r}'; \varepsilon_{\mathbf{k}m}) \psi_{\mathbf{k}m}(\mathbf{r}') \quad (20)$$

$$= (4\pi e^2/V) \sum_{\mathbf{q}, n} \sum_{\mathbf{G}, \mathbf{G}'} M_{\mathbf{G}}^{mn}(\mathbf{k}, \mathbf{q}) \cdot [M_{\mathbf{G}'}^{mn}(\mathbf{k}, \mathbf{q})]^* \int_{\omega \in \mathbf{R}} d\omega \frac{e^{-i\omega 0^+}}{(-2\pi i) \varepsilon_{\mathbf{k}m} - \omega - \varepsilon_{\mathbf{k}+\mathbf{q}n} - i0^+} \frac{\varepsilon_{-\mathbf{G}-\mathbf{G}'}^{-1}(-\mathbf{q}; \omega)}{(\varepsilon_F - \varepsilon_{\mathbf{k}+\mathbf{q}n})} \quad (21)$$

splits up in a natural way into an exchange and a correlation part,

$$\Sigma_{\mathbf{k}m}^{\text{GWA}} = \Sigma_{\mathbf{k}m}^x + \Sigma_{\mathbf{k}m}^c, \quad (22)$$

where

$$\Sigma_{\mathbf{k}m}^x = -(4\pi e^2/V) \sum_{\mathbf{q}, n} \Theta_{\varepsilon_{\mathbf{k}+\mathbf{q}, n}} \sum_{\mathbf{G}} |M_{\mathbf{G}}^{mn}(\mathbf{k}, \mathbf{q})|^2, \quad (23)$$

$$\Sigma_{\mathbf{k}m}^c = (4\pi e^2/V) \sum_{\mathbf{q}, n} \sum_{\ell} \frac{w_{\mathbf{q}\ell}}{\varepsilon_{\mathbf{k}m} - \varepsilon_{\mathbf{k}+\mathbf{q}n} + \omega_{\mathbf{q}\ell} \cdot \sigma_{\mathbf{k}+\mathbf{q}n}} \times |D_{\ell}^{mn}(\mathbf{k}, \mathbf{q})|^2. \quad (24)$$

The following quantities were introduced:

$$\Theta_{\mathbf{k}n} = \Theta(\varepsilon_F - \varepsilon_{\mathbf{k}n}), \quad (25)$$

$$\sigma_{\mathbf{k}n} = \text{sgn}(\varepsilon_F - \varepsilon_{\mathbf{k}n}), \quad (26)$$

$$D_{\ell}^{mn}(\mathbf{k}, \mathbf{q}) = \sum_{\mathbf{G}} M_{\mathbf{G}}^{mn}(\mathbf{k}, \mathbf{q}) \phi_{-\mathbf{G}}^{\ell}(-\mathbf{q}), \quad (27)$$

$$w_{\mathbf{q}\ell} = z_{\mathbf{q}\ell} \omega_{\mathbf{q}\ell} / 2. \quad (28)$$

Starting from a given LDA band structure the GWA energies are calculated from (8) as

$$\varepsilon_{\mathbf{k}n}^{\text{GWA}} = \varepsilon_{\mathbf{k}n}^{\text{LDA}} + (\Sigma_{\mathbf{k}n}^{\text{GWA}} - \Sigma_{\mathbf{k}n}^{\text{LDA}}). \quad (29)$$

The numerical evaluation of these formulas involves integrations over the Brillouin zone,

$$\frac{1}{V} \sum_{\mathbf{q}} = \frac{1}{(2\pi)^3} \int_{V_{\text{BZ}}} d^3q. \quad (30)$$

They are performed in a *special point* summation scheme.²⁵⁻²⁷ The basic idea of this integration scheme is the division of the Brillouin zone volume V_{BZ} into N volumes V_i of equal size leading to the approximation

$$\begin{aligned} \frac{1}{V_{\text{BZ}}} \int_{V_{\text{BZ}}} d^3q f(\mathbf{q}) &= \frac{1}{N} \sum_i \frac{1}{V_{\text{BZ}}/N} \int_{V_i} d^3q f(\mathbf{q}) \\ &\approx \frac{1}{N} \sum_i f(\mathbf{q}_i) \end{aligned} \quad (31)$$

with $\mathbf{q}_i \in V_i$. This method will of course only give good results for finite N if the function $f(\mathbf{q})$ is well behaved. However, the functions $M_{\mathbf{G}=\mathbf{0}}^{mn}(\mathbf{k}, \mathbf{q})$ and $D_{\ell}^{mn}(\mathbf{k}, \mathbf{q})$ and also their absolute squares diverge for $\mathbf{q} \rightarrow \mathbf{0}$ according to

$$M_{\mathbf{G}=\mathbf{0}}^{mn}(\mathbf{k}, \mathbf{q} \approx \mathbf{0}) \approx (1 - \delta_{mn}) \sum_{i=1}^3 \frac{q_i}{|\mathbf{q}|} C_i^{mn}(\mathbf{k}) + \frac{\delta_{mn}}{|\mathbf{q}|}. \quad (32)$$

Therefore prescription (31) has to be modified: Replacing the function by an analytically known approximation,

$$f(\mathbf{q}) \approx \tilde{f}(\mathbf{q}), \quad (33)$$

the integration over the critical volume V_0 can be easily performed:

$$\begin{aligned} \frac{1}{V_{\text{BZ}}} \int_{V_{\text{BZ}}} d^3q f(\mathbf{q}) &\approx \frac{1}{N} \sum_{i (\neq 0)} f(\mathbf{q}_i) \\ &+ \frac{1}{V_{\text{BZ}}/N} \int_{V_0} d^3q \tilde{f}(\mathbf{q}). \end{aligned} \quad (34)$$

It is this integration which is treated in this work with much more care than in previous work.^{4,5} The GWA results presented here are therefore of better numerical quality.

Substituting $M_{\mathbf{G}=\mathbf{0}}^{mn}(\mathbf{k}, \mathbf{q})$ in the volume V_0 around $\mathbf{q} \approx \mathbf{0}$ by the approximation (32) in the evaluation of the self-energy in (21) and of the dielectric matrix in (12)–(15) and replacing all other (continuous) functions by their value at $\mathbf{q} = \mathbf{0}$ in V_0 we are left with integrals of the form

$$a = \frac{1}{V_{\text{BZ}}/N} \int_{V_0} d^3q \left(1 / \sum_{r,s=1}^3 q_r A_{rs} q_s \right), \quad (35)$$

$$b_{ij} = \frac{1}{V_{\text{BZ}}/N} \int_{V_0} d^3q \left(q_i q_j / \sum_{r,s=1}^3 q_r A_{rs} q_s \right). \quad (36)$$

These can be transformed into *surface integrals* by the Gauss integral theorem. By a suitable choice of the position of V_0 , $\mathbf{q} = \mathbf{0}$ lies in the center of V_0 and the surface integrals do not cause any numerical difficulty.

Starting from the idea of the Brillouin zone the natural choice for the shape of the volume elements should be smaller copies of the Brillouin zone. For numerical purposes we prefer to start from an equivalent primitive cell of the reciprocal lattice with the shape of a parallelepiped subdividing it into smaller parallelepipeds of the same shape. The crystal symmetry can be regained by averaging over all nonequivalent parallelepipeds generated by all rotational symmetries of the system.

With this choice of V_0 the required integrations over the Brillouin zone of the form (34) are performed with much greater numerical accuracy than the procedure of Phillips and Kleinman²⁸ of spherical averaging used by Hybertsen and Louie⁴ and Godby, Schlüter, and Sham.⁵ The numerical quality of this procedure had already been criticized by Gygi and Baldereschi²⁹ who found deviations compared to their own integration scheme as big as 1 eV.

As a side product this method allows for the calculation of the Hartree-Fock band structure. Since the Hartree-Fock wave functions in solids are similar to the LDA wave functions,³⁰

$$\psi_{\mathbf{k}n}^{\text{HFA}}(\mathbf{r}) \approx \psi_{\mathbf{k}n}^{\text{LDA}}(\mathbf{r}) \quad (37)$$

the energies $\epsilon_{\mathbf{k}n}^{\text{HFA}}$ can be calculated using only the exchange contribution (23) to the GWA self-energy (22).

This leads to the approximation of the Hartree-Fock energies:⁶

$$\epsilon_{\mathbf{k}n}^{\text{HFA}} \approx \epsilon_{\mathbf{k}n}^{\text{LDA}} - \Sigma_{\mathbf{k}n}^{\text{LDA}} + \Sigma_{\mathbf{k}n}^x \quad (38)$$

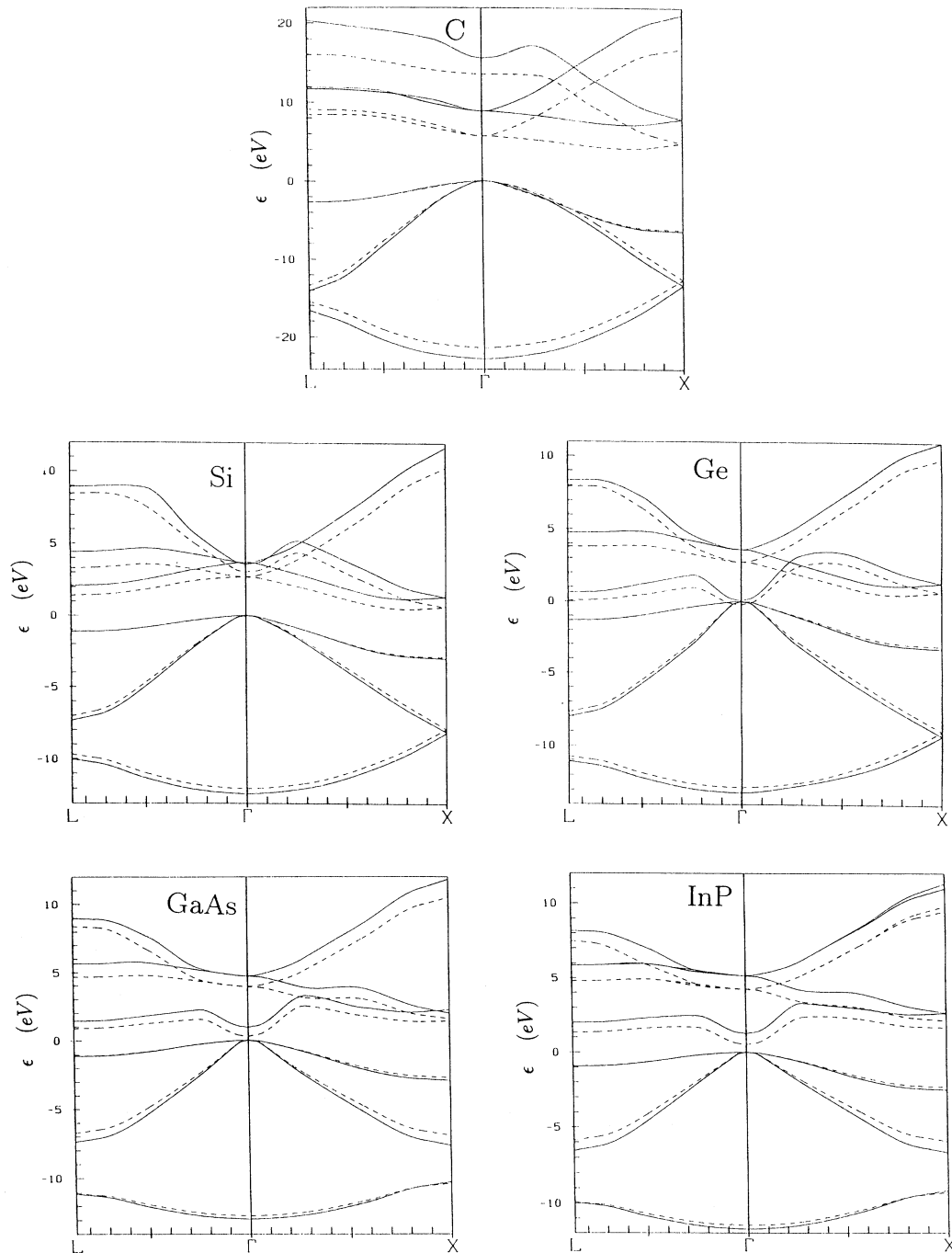


FIG. 1. Calculated electronic band structure (neglecting spin-orbit splitting) along lines of high symmetry for diamond, silicon, germanium, gallium arsenide, and indium phosphide. The dashed line shows the LDA band structure calculated by Schmid and Christensen (Ref. 31). The solid line shows the GWA band structure resulting from the addition of these LDA energies and the GWA corrections calculated in this work.

TABLE I. Calculated electronic energies (neglecting spin-orbit splitting) at points of high symmetry for diamond. The LDA energies were calculated by Schmid and Christensen (Ref. 31). The GWA band structure results from the addition of these LDA energies and the GWA corrections calculated in this work. The experimental values are taken from Ref. 38 (a), Ref. 31 (b), and Ref. 39 (c).

	\mathbf{k}	m	ϵ^{LDA}	ϵ^{GWA}	ϵ^{expt}	
diamond	Γ	8	13.50	15.53	15 a	
		5-7	5.66	8.84	7.4 a	
		2-4	0.00	0.00	0.00	
		1	-21.39	-22.77	-21 b	
	L	8	16.01	20.27		
		6,7	8.35	11.85		
		5	9.03	11.66		
		3,4	-2.77	-2.78	-3 b	
		2	-13.47	-14.19	-13 b	
		1	-15.56	-16.72	-16 b	
	X	7,8	16.70	21.02		
		5,6	4.78	7.86	6.0 b	
		3,4	-6.34	-6.51	-5 b	
		1,2	-12.69	-13.43	-13 b	
		ϵ_{gap}	$E_{\Gamma} - E_{0.7\mathbf{k}_{\Gamma X}}$	4.17	7.16	5.48 c

IV. RESULTS

The method described in the previous section was applied to diamond, silicon, germanium, gallium arsenide, and indium phosphide. The EPM band structure based on the parametrization of Cohen and co-workers^{17,18} was used. 89 reciprocal-lattice vectors turned out to be sufficient for a good convergence. The energies have been obtained using the extrapolation of \mathbf{k} meshes equivalent

to 64, 216, and 343 points in the Brillouin zone to the limit of an infinitely fine mesh. The extrapolated energies differed only by less than 0.05 eV from the corresponding value of the 343-point mesh. The only exception in this good convergence was the exchange part of the self-energy of the lowest conduction band in Ge with Γ_2' symmetry. A \mathbf{k} mesh equivalent to 1000 in the Brillouin zone had to be used to reach the same accuracy. This state had already been the issue of longer discussion:⁴ It is of

TABLE II. Calculated electronic energies (neglecting spin-orbit splitting) at points of high symmetry for silicon. The LDA energies were calculated by Schmid and Christensen (Ref. 31). The GWA band structure results from the addition of these LDA energies and the GWA corrections calculated in this work. All experimental values are taken from Ref. 39.

	\mathbf{k}	m	ϵ^{LDA}	ϵ^{GWA}	ϵ^{expt}	
Si	Γ	8	3.02	3.55	4.15(5)	
		5-7	2.68	3.68	3.35	
		2-4	0.00	0.00	0.00	
		1	-12.03	-12.38	-12.5(6)	
	L	8	8.42	8.90		
		6,7	3.26	4.38	3.91	
		5	1.38	2.06	2.04(6)	
		3,4	-1.17	-1.15	-1.2(2)	
		2	-7.10	-7.39	-6.8(2)	
		1	-9.72	-10.04	-9.3(4)	
	X	7,8	10.27	11.67		
		5,6	0.62	1.33	1.13	
		3,4	-2.89	-2.99	-2.9	
		1,2	-7.91	-8.15		
		ϵ_{gap}	$E_{\Gamma} - E_{0.85\mathbf{k}_{\Gamma X}}$	0.50	1.21	1.17

TABLE III. Calculated electronic energies (neglecting spin-orbit splitting) at points of high symmetry for germanium. The LDA energies were calculated by Schmid and Christensen (Ref. 31). The GWA band structure results from the addition of these LDA energies and the GWA corrections calculated in this work. All experimental values are taken from Ref. 39.

	\mathbf{k}	m	ϵ^{LDA}	ϵ^{GWA}	ϵ^{expt}	
Ge	Γ	6-8	2.74	3.60	3.25	
		5	-0.24	0.06	1.0	
		2-4	0.00	0.00	0.00	
		1	-12.86	-13.16	-12.56	
	L	8	7.88	8.30		
		6,7	3.76	4.73	4.30	
		5	0.02	0.59	0.86	
		3,4	-1.37	-1.36	-1.43	
		2	-7.75	-8.06	-7.51	
		1	-10.79	-11.12	-10.29	
	X	7,8	9.80	10.96		
		5,6	0.68	1.31	1.26	
		3,4	-3.10	-3.26	-3.19	
		1,2	-9.00	-9.31	-8.55	
		ϵ_{gap}	$\Gamma - L$	0.02	0.59	0.86

almost pure s character and has all of its weight localized on the ion cores. This makes it a problematic case for any pseudopotential calculation.

A big reduction in computation time was reached by using the crystal symmetries developing an extension of the usual special point scheme.²⁷ The computation of all dielectric matrices with 89 reciprocal-lattice vector indices necessary in the case of the \mathbf{k} mesh equivalent to

343 points requires only about 40 min on a Cray XMP computer. The evaluation of the self-energies takes another 15 min. This allowed for the use of the \mathbf{k} mesh equivalent to 1000 points in the Brillouin zone for the exchange energy in Ge.

Figure 1 shows the LDA band structure of Schmid and Christensen³¹ calculated with the scalar-relativistic linear muffin-tin-orbital (LMTO) method,³² as previously

TABLE IV. Calculated electronic energies (neglecting spin-orbit splitting) at points of high symmetry for gallium arsenide. The LDA energies were calculated by Schmid and Christensen (Ref. 31). The GWA band structure results from the addition of these LDA energies and the GWA corrections calculated in this work. The experimental values are taken from Ref. 39 (c) and Ref. 41 (d).

	\mathbf{k}	m	ϵ^{LDA}	ϵ^{GWA}	ϵ^{expt}	
GaAs	Γ	6-8	3.91	4.72	4.716 c	
		5	0.26	0.93	1.632 c	
		2-4	0.00	0.00	0.00 c	
		1	-12.71	-12.94	-13.1 c	
	L	8	8.36	8.95		
		6,7	4.65	5.63	5.6 d	
		5	0.84	1.40	1.85 c	
		3,4	-1.11	-1.13	-1.20 c	
		2	-6.76	-7.41	-6.70 c	
		1	-11.10	-11.14	-11.24 c	
	X	7,8	10.45	11.79		
		6	1.39	2.24	2.50 c	
		5	1.58	1.99	2.18 c	
		3,4	-2.70	-2.89	-2.80 c	
		2	-6.92	-7.64	-6.70 c	
		1	-10.39	-10.28	-10.75 c	
		ϵ_{gap}	$\Gamma - \Gamma$	0.26	0.93	1.632 c

applied also to semiconductors.³³⁻³⁷ The GWA energies result from adding the calculated energy corrections. Tables I-V list the energies calculated at points of high symmetry of the zinc-blende structure. The top valence band

at Γ is chosen as zero energy for all band structures.

For the valence bands the LDA energies show good agreement with the experimental values. The GWA corrections give more or less the same shift for all valence

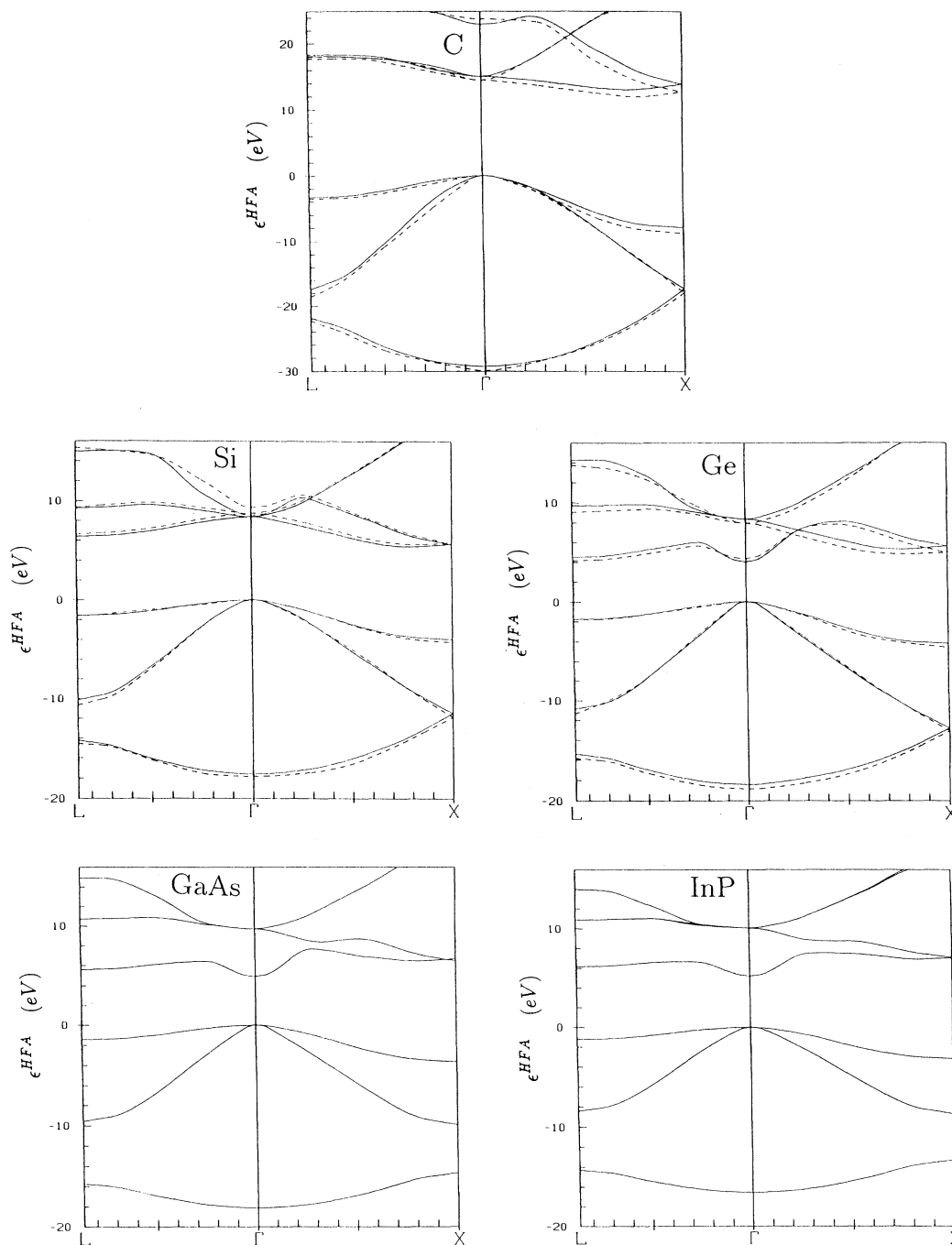


FIG. 2. Calculated Hartree-Fock band structure along lines of high symmetry for diamond, silicon, germanium, gallium arsenide, and indium phosphide. The dashed line shows the results of a Hartree-Fock calculation of Svane and Andersen (Ref. 38) using the tight-binding LMTO scheme. The solid line shows the Hartree-Fock band structure resulting from the addition of the LDA energies calculated by Schmid and Christensen (Ref. 31) and the exchange corrections calculated in this work according to (38).

TABLE V. Calculated electronic energies (neglecting spin-orbit splitting) at points of high symmetry for indium phosphide. The LDA energies were calculated by Schmid and Christensen (Ref. 31). The GWA band structure results from the addition of these LDA energies and the GWA corrections calculated in this work. The experimental values are taken from Ref. 39 (c), Ref. 34 (e), and Ref. 42 (f).

	\mathbf{k}	m	ϵ^{LDA}	ϵ^{GWA}	ϵ^{expt}	
InP	Γ	6-8	4.21	5.17	5.00 f	
		5	0.50	1.23	1.460 c	
		2-4	0.00	0.00	0.00	
		1	-11.50	-11.75	-11.6 e	
	L	8	7.47	8.17		
		6,7	4.75	5.85	5.68 e	
		5	1.30	1.97	2.32 e	
		3,4	-0.94	-0.94	-0.98 e	
		2	-5.90	-6.56	-5.93 e	
		1	-9.94	-9.97	-9.89 e	
	X	8	9.79	11.28		
		7	9.45	10.94		
		6	2.10	2.63	2.92 e	
		5	1.64	2.60	2.42 e	
		3,4	-2.34	-2.52	-2.40 e	
		2	-5.94	-6.60	-5.93 e	
		1	-9.29	-9.16	-9.24 e	
		ϵ_{gap}	$\Gamma - \Gamma$	0.50	1.23	1.46 c

bands which results in a small shift of the GWA energies. The exception is the second valence band in heteropolar GaAs and InP which is pushed to lower energies in contrast to the experimental values which agree excellently with the corresponding LDA values.

For the conduction bands GWA leads generally to an improvement with respect to LDA. Nevertheless the agreement with experiment is far from perfect. The most obvious failure is the lowest conduction state in Ge with Γ'_2 symmetry which had already been mentioned because of its convergency problems. While LDA predicts a negative gap of -0.24 eV the GWA corrections are just enough to shift this band 0.06 eV above the valence bands, leaving it 1 eV below its experimental value. In contrast to this the experimental indirect band gap is reproduced quite well.

Figure 2 shows the Hartree-Fock band structure derived from the GWA calculations as continuous lines in comparison with the results of a Hartree-Fock calculation of Svane and Andersen³⁸ shown as dashed lines. The agreement is reasonably good.

V. COMPARISON WITH PREVIOUS WORK

The data presented here can claim to stand on more solid ground than former GWA investigations. The EPM wave functions are certainly more pleasant concerning their convergency behavior than the pseudofunctions from *ab initio* pseudopotential calculations. The results, however, show rather poor agreement with experiment compared to these former GWA results.^{4,5} This unanticipated fact will be discussed below.

The calculations with the well-behaved EPM wave functions have shown that a \mathbf{k} mesh equivalent to at least 216 points in the Brillouin zone is required to obtain well-converged results. The calculations of Godby, Schlüter, and Sham⁵ employ a \mathbf{k} mesh which is equivalent to 27 points in the Brillouin zone, extrapolating these data to a \mathbf{k} mesh equivalent to 64 points. Therefore they may not have converged yet.

Hybertsen and Louie⁴ checked the convergence of their results with respect to this point using \mathbf{k} meshes equivalent to 8, 64, and 216 points in the Brillouin zone. This proved to be enough in our calculations as well except for the lowest conduction state in Ge with Γ'_2 symmetry. Nevertheless by means of the improved integration scheme the results published here should be more accurate.

The method of von der Linden and Horsch had been the basis for the GWA calculations of this work. The difference from this work is their use of a model dielectric function and of another Brillouin-zone integration scheme. The model dielectric function did *not* reproduce the actual random-phase approximation dielectric function which has to be used in the GWA. In addition the integration scheme also does not seem to be sufficiently accurate.

VI. SUMMARY

In this paper a method is presented for the calculation of the energy corrections of GWA with respect to LDA. Using well-converged LDA band structures the GWA band structures of diamond, silicon, germanium, gallium arsenide, and indium phosphide have been calculated.

The overall agreement with experiment is quite good but by no means perfect. The use of an EPM band structure as input is not absolutely satisfactory and could be one reason for the discrepancies. Nevertheless even the use of pseudofunctions from an *ab initio* pseudopotential calculation cannot prevent considerable errors as was shown for Ge. The experience with GWA calculations from this work shows that the additional technical approximations are still not developed sufficiently to produce absolutely reliable GWA results. Questions about the possibility of the GWA to explain certain physical phenomena³⁹ can therefore not be answered yet.

ACKNOWLEDGMENTS

I am very grateful to P. Fulde for his help and encouragement for this work. I would like to thank U. Schmid and S. Zollner for encouraging me to write this paper. I am obliged to U. Schmid and N. E. Christensen for providing me with the LDA band-structure data and to W. von der Linden for introducing me into the topic and providing me with his computer codes. I thank G. Zwicknagl, A. Kaiser, and N. E. Christensen for carefully reading this paper and P. Horsch for discussions.

*Present address: Gesellschaft für Angewandte Supraleitung, c/o Kernforschungszentrum Karlsruhe, P.O. 3640 D-7500 Karlsruhe 1, FRG.

¹P. Hohenberg and W. Kohn, Phys. Rev. **136**, B864 (1964).

²W. Kohn and L. J. Sham, Phys. Rev. **140**, A1133 (1965).

³G. B. Bachelet and N. E. Christensen, Phys. Rev. B **31**, 879 (1984).

⁴M. S. Hybertsen and S. G. Louie, Phys. Rev. B **34**, 5390 (1986).

⁵R. W. Godby, M. Schlüter, and L. J. Sham, Phys. Rev. B **37**, 10 159 (1988).

⁶W. von der Linden and P. Horsch, Phys. Rev. B **37**, 8351 (1988).

⁷J. C. Inkson, *Many-Body Theory of Solids* (Plenum, New York, 1984).

⁸U. von Barth and L. Hedin, J. Phys. C **5**, 1629 (1972).

⁹D. M. Ceperley and B. J. Alder, Phys. Rev. Lett. **45**, 566 (1980).

¹⁰J. P. Perdew and A. Zunger, Phys. Rev. B **23**, 5048 (1981).

¹¹M. Rasolt and S. H. Vosko, Phys. Rev. **10**, 4195 (1974).

¹²M. Rasolt, S. B. Nickerson, and S. H. Vosko, Solid State Commun. **16**, 827 (1975).

¹³L. Hedin, Phys. Rev. **139**, A796 (1965).

¹⁴L. Hedin and S. Lundqvist, *Solid State Physics: Advances in Research and Applications* (Academic, New York, 1969), Vol. 23.

¹⁵G. Strinati, H. J. Mattausch, and W. Hanke, Phys. Rev. B **25**, 2867 (1982).

¹⁶D. R. Hamann, M. Schlüter, and C. Chiang, Phys. Rev. Lett. **43**, 1494 (1979).

¹⁷M. Cohen and T. K. Bergstresser, Phys. Rev. **141**, 789 (1966).

¹⁸W. Saslow, T. K. Bergstresser, and M. Cohen, Phys. Rev. Lett. **16**, 354 (1966).

¹⁹S. L. Adler, Phys. Rev. **126** (1962) 413.

²⁰N. Wiser, Phys. Rev. **129**, 62 (1963).

²¹A. Baldereschi and E. Tosatti, Solid State Commun. **29**, 131 (1979).

²²R. Car, E. Tosatti, S. Baroni, and S. Leelaprute, Phys. Rev. B **24**, 985 (1981).

²³D. L. Johnson, Phys. Rev. B **9**, 4475 (1974).

²⁴The ω_{ql} can all be shown to be real (Ref. 6) contrary to the plasmon-pole frequencies used in the ansatz of Hybertsen and Louie. In addition, far fewer parameters are required in the plasmon-pole approximation of von der Linden and Horsch because only the eigenvalues and not each matrix element is parametrized by a plasmon-pole function.

²⁵A. Baldereschi, Phys. Rev. B **7**, 5212 (1973).

²⁶D. J. Chadi and M. L. Cohen, Phys. Rev. B **8**, 5747 (1973).

²⁷H. J. Monkhorst and J. D. Pack, Phys. Rev. B **13**, 5188 (1976).

²⁸J. C. Phillips and L. Kleinman, Phys. Rev. **128**, 2098 (1962).

²⁹F. Gygi and A. Baldereschi, Phys. Rev. B **34**, 4405 (1986).

³⁰W. von der Linden, P. Fulde, and K. P. Bohnen, Phys. Rev. B **34**, 1063 (1986).

³¹U. Schmid and N. E. Christensen (private communication).

³²O. K. Andersen, Phys. Rev. B **12**, 3060 (1975).

³³M. Cardona and N. E. Christensen, Solid State Commun. **58**, 421 (1986).

³⁴M. Cardona, N. E. Christensen, and G. Fasol, Phys. Rev. B **38**, 1806 (1988).

³⁵U. Schmid, N. E. Christensen, and M. Cardona, Phys. Rev. B **41**, 5919 (1990).

³⁶S. Zollner, U. Schmid, N. E. Christensen, and M. Cardona, Appl. Phys. Lett. **57**, 22 (1990).

³⁷N. E. Christensen, S. Satpathy, and Z. Pawlowska, Phys. Rev. B **36**, 1032 (1987).

³⁸A. Svane and O. K. Andersen, Phys. Rev. B **34**, 5512 (1986).

³⁹R. W. Godby and R. J. Needs, Phys. Rev. Lett. **62**, 1169 (1989).

⁴⁰M. S. Hybertsen and S. G. Louie, Phys. Rev. B **34**, 2920 (1986).

⁴¹*Intrinsic Properties of Group IV Elements and III-V, II-VI, and I-VII Compounds*, Landolt-Börnstein, New Series, Vol. 22 (Springer, Berlin, 1987).

⁴²P. Lautenschlager, M. Garriga, S. Logothetidis, and M. Cardona, Phys. Rev. B **35**, 9174 (1987).

⁴³D. E. Aspnes and A. A. Studna, Phys. Rev. B **7**, 4605 (1973).

⁴⁴P. Lautenschlager, M. Garriga, and M. Cardona, Phys. Rev. B **36**, 4813 (1987).